DOI: 10.2478/s11686-008-0054-3

Acta Parasitologica, 2008, 53(4), 330–338; ISSN 1230-2821

VERSITA

Myxobolus species infecting the cartilaginous rays of the gill filaments in cyprinid fishes

Kálmán Molnár*, Gábor Cech and Csaba Székely

Veterinary Medical Research Institute, Hungarian Academy of Sciences, PO Box 18, H-1518 Budapest, Hungary

Abstract

During a survey on myxosporean parasites of cyprinid fishes in Hungary, *Myxobolus* infections were found in the cartilaginous rays of the gill filaments in roach (*Rutilus rutilus*) and bleak (*Alburnus alburnus*). *Myxobolus* spp. causing the infections were studied by morphological, histological and molecular methods. Small plasmodia surrounded by chondrocytes contained relatively few spores which differed from each other and from the known *Myxobolus* spp. both in their morphology and 18S rDNA sequences. Both species, described as *M. feisti* sp. nov. and *M. susanlimae* sp. nov., are characterised by a specific cartilaginous histotropism.

Keywords

Myxozoa, new species, histology, site selection, molecular phylogeny

Introduction

The numerous *Myxobolus* spp. infecting fishes are characterised by a specific organ and tissue tropism, and their plasmodia have well-defined predilections for their site of development (Molnár 1994). Several species select cartilaginous tissues as the site of plasmodial development. Longshaw *et al*. (2003) listed 13 *Myxobolus* species developing typically in the cartilage. The best known chondrophilic species is *Myxobolus cerebralis* Hofer, 1903 infecting salmonids and causing whirling disease with heavy losses (Schäperclaus 1931, Hoffman *et al*. 1962). Similar intensive infections are caused in cartilaginous elements by *M. cartilaginis* (Hoffman, Putz et Dunbar, 1965) and *M. buckei* Longshaw, Frear et Feist, 2003. All these species, however, have different sites of predilection in the cartilage. While *M. cerebralis* develops mostly in the head cartilage of salmonids, *M. cartilaginis* prefers the gill arches of the centrarchid *Lepomis* spp. and *M. buckei* forms plasmodia in the vertebrae of leuciscine cyprinids. No papers have been published on *Myxobolus* infections of the cartilaginous rays of gill filaments. However, a picture has been presented by Nowak *et al*. (2001) on the infection of this location in the gills of the roach.

In this paper we report on the occurrence of two *Myxobolus* spp. infecting the cartilaginous gill rays of fish and describe them as *M. feisti* sp. nov. and *M. susanlimae* sp. nov. from the roach (*Rutilus rutilus*) and the bleak (*Alburnus alburnus*), respectively.

Materials and methods

The fish material showing infection in the cartilaginous gill rays was obtained from Hungarian lakes and rivers. In Hungary there has been a long-term project for surveying the health condition of wild fishes. In the framework of this programme, parasitic infections of economically important and some commonly occurring fish species have been studied. Most of the fish studied originated from Lake Balaton, from the Kis-Balaton water reservoir and from reaches of the River Danube north of Budapest. In most cases a complete parasitological examination was performed, but specific investigations on infections involving the cartilaginous rays of gill filaments were also carried out in 2005 and 2007.

Altogether 119 specimens of roach (*Rutilus rutilus* L.), 95 from Lake Balaton and 24 from the Kis-Balaton water reservoir, were examined. The total length of 4-month- to 5-year-old roach varied from 4 to 26 cm. Of bleak (*Alburnus alburnus* L.), 152 specimens from Lake Balaton and 63 specimens from the River Danube were studied. The length of 1- to 4-year-old fish varied from 4 to 11 cm. Fish were seined, carried to the laboratory alive in oxygenated plastic bags, and kept in aquaria. Fish given a cervical cut were examined within 4 days of capture. Before extermination fish were sedated by clove oil. Within a complete parasitological examination the hemibranchia of the gills and the fins were cut and examined under a dissecting microscope for the presence of *Myxobolus* plasmodia. Pieces from the kidneys, liver, spleen,

*Corresponding author: molnar@vmri.hu

testes and muscles were compressed between two glass plates, and examined first under a stereomicroscope, then at 200- to 400-fold magnification in a Zeiss compound microscope. The gut was first surveyed under a dissecting microscope as a whole, then it was cut open and compressed between two glass plates. *Myxobolus* spores from the isolated and opened cysts were first studied in a wet mount, and then some of the spores were placed in glycerine-jelly onto a slide under a cover slip and preserved as a reference slide. Other spore samples were collected into Eppendorf tubes and stored at –20°C for later molecular taxonomy. Tissue samples from infected organs containing developing and mature plasmodia were fixed in Bouin's solution, embedded in paraffin wax, cut to 4–5 µm sections, and stained with haematoxylin and eosin. The vitality of spores was checked by adding spores into a 0.4% solution of urea. Spores of a given plasmodium were regarded as mature when at least 90% of the spores extruded polar filaments in that solution. Unfixed spores were studied by Nomarski differential interference contrast of an Olympus BH2 microscope. Fresh spores were photographed with an Olympus DP10 digital camera or recorded on videotapes; digitised images were obtained and measurements were taken with the IMAGO® software. All measurements are given in µm.

Molecular methods

For DNA extractions, spore samples preserved in ethanol were centrifuged at 5000 × *g* for 5 min to pellet the myxospores, then the ethanol was removed. The DNA was extracted using a QIAGEN DNeasy™ tissue kit (animal tissue protocol, Qiagen) and eluted in 50 µl of buffer AE.

The 18S rDNA was amplified using the primers 18e and 18g' (Table I) in a 25 µl reaction mixture, which comprised 1 µl extracted genomic DNA, 5 µl 1mM deoxyribonucleotide triphosphates (dNTPs, MBI Fermentas), 0.25 µl of each primer, 2.5 µl 10X Taq buffer (MBI Fermentas), 1.25 µl 25 mM $MgCl_2$, 1 µl Taq polymerase (2 U) (MBI Fermentas) and 12 µl DEPC water. The PCR cycle consisted of an initial denaturation step of 94°C for 4 min, followed by 35 cycles of 94°C for 50 s, 56°C for 50 s, 72°C for 80 s and finished with terminal extension at 72°C for 7 min, then rested at 4°C.

This was followed by a second round of PCR with the SphF-SphR primer pair (Table I). The total volume of the nested PCR reactions was 50 µl, which contained 1 µl amplified DNA, 10 µl 1 mM deoxyribonucleotide triphosphates (dNTPs, MBI Fermentas), 0.5 µl of each primer, 5 µl 10X Taq buffer (MBI Fermentas), 2.5 µl 25 mM $MgCl_2$, 2 µl Taq polymerase (2 U) (MBI Fermentas) and 28.5 µl DEPC water. Amplification conditions in the second round were: 94°C for 50 s, 56°C for 50 s, 72°C for 60 s for 35 cycles, and the cycle was terminated with an extension period at 72°C for 10 min, and then rested at 4°C. Both PCR cycles were performed in a PTC-200 thermocycler (MJ Research). The PCR products were electrophoresed in 1.0% agarose gels in Tris-Acetate-EDTA (TAE) buffer gel stained with 1% ethidium bromide and then purified with the PCR-M™ Clean Up System (Viogene).

Purified PCR products were sequenced in both directions with the primers SphF, SphR, MC3, MC5, MB3f, MB5r (Table I) using the ABI BigDye Terminator v3.1 Cycle Sequencing Kit with an ABI 3100 Genetic Analyser.

The various forward and reverse sequence segments were aligned in BioEdit (Hall 1999) and ambiguous bases clarified using corresponding ABI chromatograms. Nucleotide sequences were aligned with the software CLUSTAL W (Thompson *et al*. 1994). The alignment was corrected manually using the alignment editor of the software MEGA 4.0 (Tamura *et al*. 2007). DNA sequence similarities were calculated with the Sequence Identity Matrix of the software BioEdit. Phylogenetic calculations were performed with Paup* 4.0b10 (Swofford 2000). The data were analysed with maximum parsimony [close-neighbour-interchange level (CNI) 3, random addition trees 100] and maximum likelihood (transversion/transition ratio 1:2, empirical base frequencies, one rate class for nucleotide substitution and global arrangements). Also neighbour-joining was calculated by Mega 4.0 using the Tamura-Nei model and pairwise deletion for gaps. Clade support was assessed with bootstrapping (100 replicates for maximum likelihood and maximum parsimony and 1000 replicates for neighbour-joining). *Ceratomyxa shasta* was chosen as an outgroup.

Results

Myxobolus *infection in the cartilaginous gill rays of roach*

Myxobolus plasmodia in the cartilaginous rays of the gill filaments were found only in 11 roach specimens (9.2%). Infection was found in 8 fish from the Kis-Balaton water reservoir and 3 fish from Lake Balaton. It should be mentioned that rare cases of infection with this species had already been found

Table I. Primers used for PCR or sequencing

Primer	Sequence	Source
18e	5'-CTG GTT GAT TCT GCC AGT-3'	Hillis and Dixon (1991)
18g'	5'-CGG TAC TAG CGA CGG GCG GTG TG-3'	Hillis and Dixon (1991)
SphF	5'-ACT CGT TGG TAA GGT AGT GGC T-3'	Eszterbauer and Székely (2004)
SphR	5'-GTT ACC ATT GTA GCG CGC GT-3'	Eszterbauer and Székely (2004)
MC5	5'-CCT GAG AAA CGG CTA CCA CAT CCA-3'	Molnár *et al*. (2002)
MC3	5'-GAT TAG CCT GAC AGA TCA CTC CAC A-3'	Molnár *et al*. (2002)
MB5r	5'-ACC GCT CCT GTT AAT CAT CAC C-3'	Eszterbauer (2004)
MB5f	5'-GAT GAT TAA CAG GAG CGG TTG G-3'	Eszterbauer (2004)

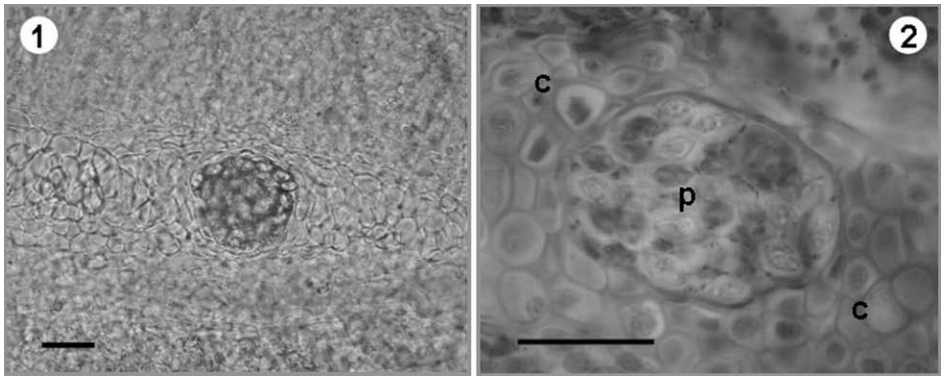

Figs 1–2. *Myxobolus feisti* sp. nov. plasmodium in a cartilaginous gill ray of the roach. Scale bar = 25 µm (**1**). Cross-section of a *Myxobolus feisti* sp. nov. plasmodium located in a cartilaginous ray of the gill filament in the roach. Spores in the plasmodium (p) are surrounded by chondrocytes (c). H and E. Scale bar = 25 µm (**2**)

several years earlier. All infections were recorded in >1-year-old roach specimens harvested in late summer. In these roach specimens, small round-shaped plasmodia with a diameter of 50 to 60 µm, containing up to 500 spores were found in the gill rays surrounded by cartilage cells (Figs 1 and 2). During examination under stereomicroscope, small thickenings of the cartilage of the gill rays called attention to infection. In severe cases, 30 to 50 plasmodia were recorded in the middle part of the filaments or close to the tip. In some cases a single gill ray harboured two or three plasmodia. In milder infections with 2 to 5 plasmodia in the hemibranchium, the infection could only be observed under a compound microscope by checking the filaments cut from the gill arch and compressed between glass plates.

***Myxobolus feisti* sp. nov.** (Figs 3a-c; 4)

Description: Mature plasmodia with disporoblastic pansporoblasts were round or ellipsoidal, up to 60 in size. Spores (Figs 3a; 4) were ellipsoidal in frontal view. In sutural view they were lens-shaped (Fig. 3b). Length of the spores was 11.7 ± 0.93 (11.5–13.2) (n = 50), width 10 ± 0.77 (9.4–10.8) (n = 50), thickness 6.7 ± 0.19 (6.6–7) (n = 11). Polar capsules were pyriform, equal in size, slightly converging anteriorly, 6.2 ± 0.14 (6.0–6.3) long (n = 50) and 3.7 ± 0.22 (3.3–4) wide (n = 50). Six filament coils arranged perpendicular to the capsule length wound densely in the polar capsule. There was a large, triangular, 2.0 ± 0.32 (1.8–2.4) (n = 50) intercapsular appendix in the spores. Sutural protrusion formed a circular rim around the spore emerging about 0.8 to 1.4 over the surface of the spore (Fig. 3c). In sutural view this rim protruded over the surface of the spore 1.4 ± 0.11 (1.3–1.5) (n = 7) to 1.2 at the anterior pole, and 0.8 ± 0.20 (0.6–1.0) at the posterior pole. The thickness of the rim measured about 0.7 in sutural view. Sutural edge markings (5 to 7) were well visible in fresh spores. There was a single binucleated sporoplasm with a round iodinophilous vacuole present in the spore. Mucous envelope was not found.

Type host: Roach, *Rutilus rutilus* L. (Cyprinidae).

Type locality: Kis-Balaton water reservoir, Hungary (46°36´–46°40´N, 17°08´–17°10´E).

Other locality: Lake Balaton (46°42´–47°03´N, 17°14´–18°19´E).

Site of tissue development: Cartilaginous rays of the gill filaments.

Type material: Syntype spores in glycerine-jelly were deposited in the parasitological collection of the Zoological Department, Hungarian Natural History Museum, Budapest,

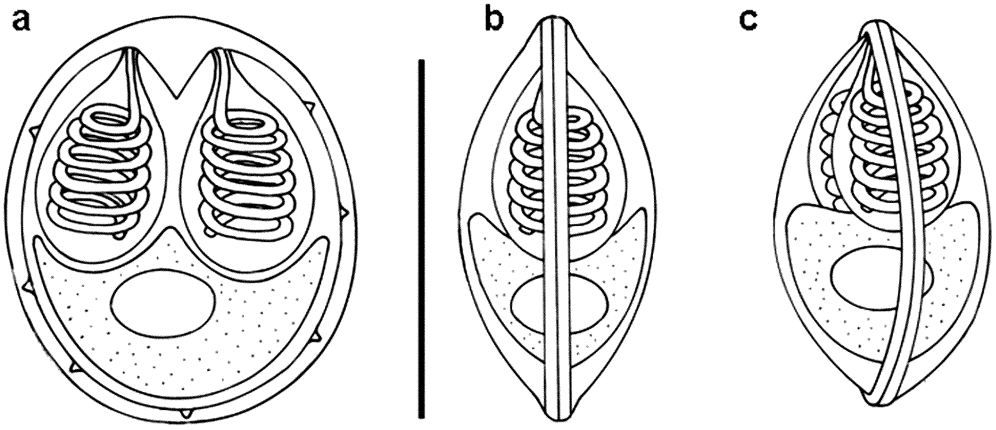

Fig. 3. Schematic drawings of *Myxobolus feisti* sp. nov. spores: a – frontal view, b – sutural view, c – semilateral view. Scale bar = 10 µm

Fig. 4. Spores of *Myxobolus feisti* sp. nov. Scale bar = 10 µm

Coll. No. HNHM-17830. The 18S rDNA sequence of *M. feisti* sp. nov. was deposited in the GenBank under the accession number EU598804.

Prevalence of infection: 44% in the >1-year-old age group.

Etymology: The species is named after Stephen Feist, the well-known British fish pathologist.

Histology of infection: Round (40–50 in diameter) or ellipsoidal (40–50 × 50–60) plasmodia filled by spores were found in the gill filaments. Plasmodia were located in the cartilaginous gill rays surrounded by chondrocytes. The spores were delimited from the chondrocytes only by a thin eosinophilic ectoplasm (Fig. 2). No major host reactions were recorded.

Molecular data: 18S rDNA sequences of four replicate samples of *M. feisti* sp. nov. (EU598804) collected from the gill rays of different roach specimens showed 100% identity on the basis of 1320 aligned base pairs. The highest genetic similarity was obtained with *M. susanlimae* sp. nov. and *M. macrocapsularis* from common bream, showing 97.2% similarity in their 18S rDNA sequences. On the phylogenetic tree (Figs 10 and 11), *M. feisti* sp. nov. also grouped with the gill parasites *M. margitae* from bleak (96.7%), *M. bramae* from common bream (95%) and *M. muelleri* from chub (94.8%).

Remarks: In its spore morphology *Myxobolus feisti* sp. nov. resembles *M. buckei* Longshaw, Frear et Feist, 2003, but the latter species has 11 to 12 coils in the polar capsule. The spores of *M. feisti* differ from the spores of *M. cartilaginis* by not having anteriorly a triangular thickening in the spore wall. Spores of *M. feisti* resemble the species *M. muelleri* Bütschli, 1892 and *M. rutili* Donec et Tozyyakova, 1984 by having ellipsoidal spores with a well-developed intercapsular appendix, but its spores are smaller than those of the latter species, and it differs from the latter species in its DNA structure as well (unpublished results of the authors).

Myxobolus *infection in the cartilaginous gill rays of bleak*

Myxobolus plasmodia in the cartilaginous rays of the gill filaments were found only in bleak specimens collected from the River Danube. All infections were recorded from 2- to 4-year-old specimens harvested in April and August. In this period 13 out of the examined 27 specimens (48%) showed infection. In these bleak specimens, small round, ellipsoidal or amorphous plasmodia 50 to 100 µm long and 50 to 60 µm wide, containing up to 1000 spores, were found in the cartilaginous gill rays surrounded by cartilage cells. Very often 2 or 3 neighbouring plasmodia grew together into a single cyst. During examination under stereomicroscope, small thickenings of the cartilage of the gill rays called attention to infection. In severe cases up to 60 plasmodia were recorded close to the tip of the gill filaments. In some cases a single gill ray harboured two or three plasmodia (Fig. 7). In milder infections with 2 to 5 plasmodia in the hemibranchium, the infection could only be observed under a compound microscope by checking the filaments cut from the gill arch and compressed between glass plates.

Table II. Comparison of spore measurements of some *Myxobolus* spp. infecting the gills of roach and bleak

***Myxobolus* spp.**	***M. feisti***	***M. buckei***	***M. muelleri***	***M. susanlimae***	***M. margitae***
Hosts	*R. rutilus*	*R. rutilus*	*R. rutilus*, *L. cephalus*	*A. alburnus*	*A. alburnus*
Spore length	11.7 ± 0.93 (11.5–13.2)	14 ± 0.7 (12.6–15.4)	9.8 ± 0.24 (9.5–10)	11.5 ± 0.22 (10.6–12)	13.7 (13–14)
Spore width	10 ± 0.77 (9.4–10.8)	11.5 ± 0.6 (10.2–12.4)	7.5 ± 0.24 (7.5–8)	9.9 ± 0.47 (9.5–10.8)	9.7 (9.5–10)
Spore thickness	6.7 ± 0.19 (6.6–7)	–	5.2 ± 0.24 (5–5.5)	9.2 ± 0.27 (8.3–10.1)	5.7 (5.5–6)
Polar capsule length	6.2 ± 0.14 (6–6.3)	6–8.6	4.6 ± 0.51 (4–5)	5.4 ± 0.16 (5.2–5.6)	5 (4.5–5.5)
Polar capsule width	3.7 ± 0.22 (3.3–4)	3.3–4.6	3.6 ± 0.5 (3–4)	3.1 ± 0.16 (2.9–3.3)	3 (2.8–3.2)
Intercapsular appendix (µm)	2.0 ± 0.32 (1.8–2.4)	large	1	1.6 ± 0.14 (1.3–1.8)	large
No. of coils in capsule	6	11–12	5–6	6	7

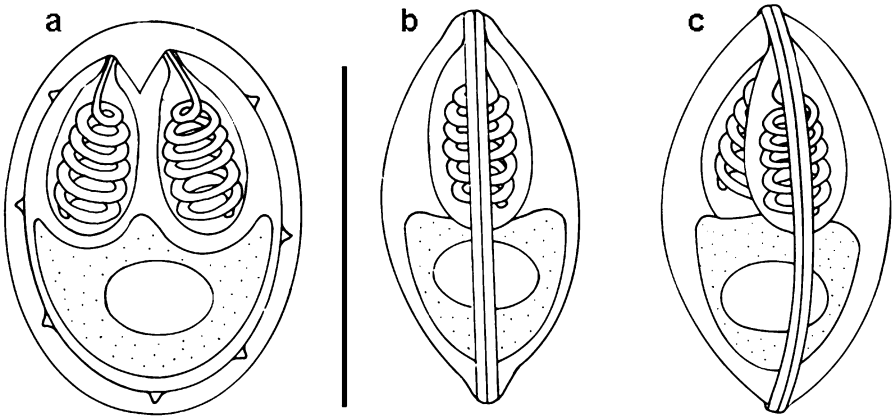

Fig. 5. Schematic drawings of *Myxobolus susanlimae* sp. nov. spores: a – frontal view, b – sutural view, c – semilateral view. Scale bar = 10 μm

***Myxobolus susanlimae* sp. nov.** (Figs 5a-c; 6–9)

Mature plasmodia with disporoblastic pansporoblasts were round, ellipsoidal or amorphous, up to 100 in size. Spores (Figs 5a; 6) were ellipsoidal in frontal view and lemon shaped in sutural view (Fig. 5b).

Length of the spores was 11.5 ± 0.219 (10.6–12.0) (n = 50), width 9.9 ± 0.47 (9.5–10.8) (n = 50), thickness 9.2 ± 0.27 (8.3–10.1) (n = 11). Polar capsules were elongated pyriform, equal in size, slightly converging anteriorly, 5.4 ± 0.16 (5.2–5.6) long (n = 50) and 3.1 ± 0.16 (2.9–3.3) wide (n = 50). Six filament coils arranged perpendicular to the capsule length wound densely in the polar capsule. There was a large, triangular, 1.6 ± 0.14 (1.3–1.8) (n = 50) intercapsular appendix in the spores. Sutural protrusion formed a circular rim around the spore emerging about 0.7 over the surface of the spore (Fig. 5c). In sutural view only slight protrusions were seen at the anterior and posterior poles. The thickness of the rim measured about 0.7 in sutural view. Sutural edge markings (No. 5 to 7) were well visible in fresh spores. There was a single binucleated sporoplasm with a round iodinophilous vacuole present in the spore. Mucous envelope was not found.

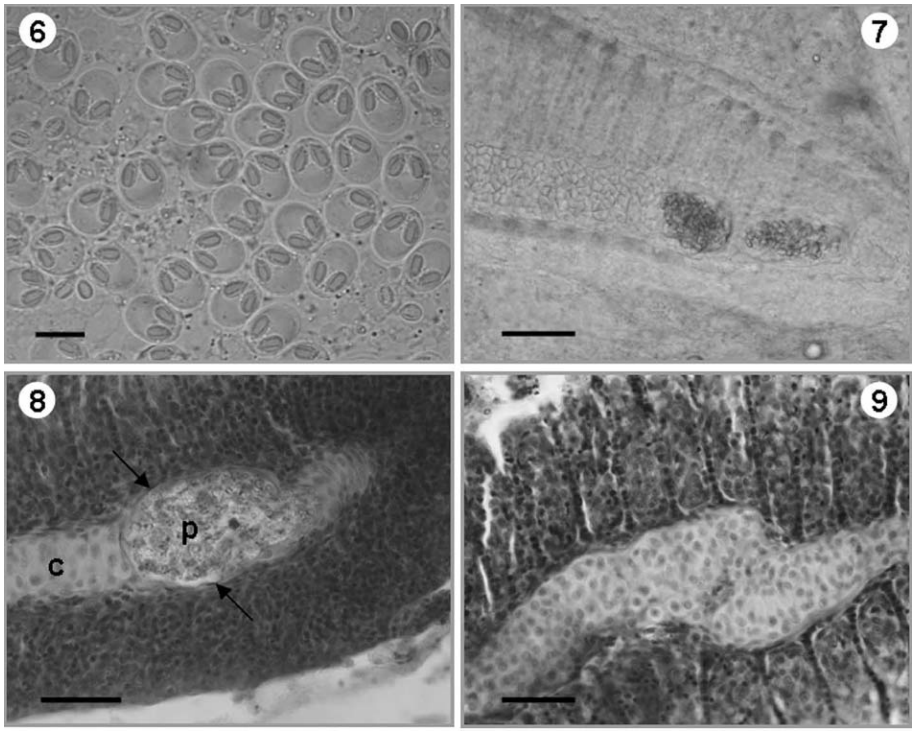

Figs 6–9. Spores of *Myxobolus susanlimae* sp. nov. (**6**). Two *M. susanlimae* sp. nov. plasmodia in a cartilaginous gill ray of bleak (**7**). Cross-section of a *M. susanlimae* plasmodium located in the cartilaginous ray of the gill filament (c) in bleak; spores in the plasmodium (p) are surrounded by perichondrial cells (arrows) H and E (**8**). Deformation of the cartilaginous gill ray due to *M. susanlimae* infection. H and E (**9**). Scale bars = 10 μm (6), 50 μm (7), 25 μm (8, 9)

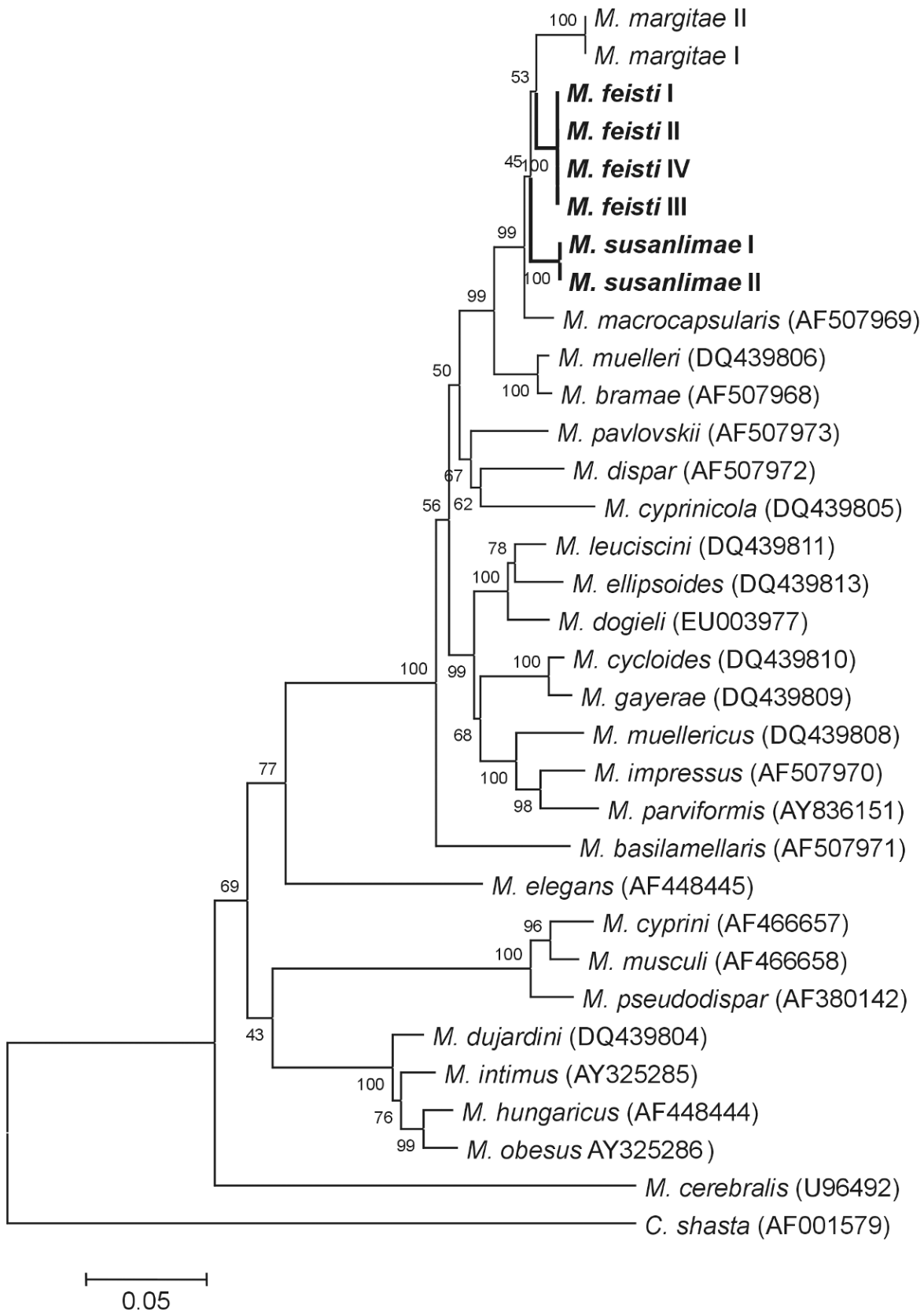

Fig. 10. Phylogenetic tree generated by neighbour-joining analyses of the 18S rDNA sequences of myxosporeans, rooted at *Ceratomyxa shasta*. Numbers at nodes indicate bootstrap confidence values (1000 replications). GenBank accession numbers are given in parentheses. Myxosporeans examined in this study are in bold

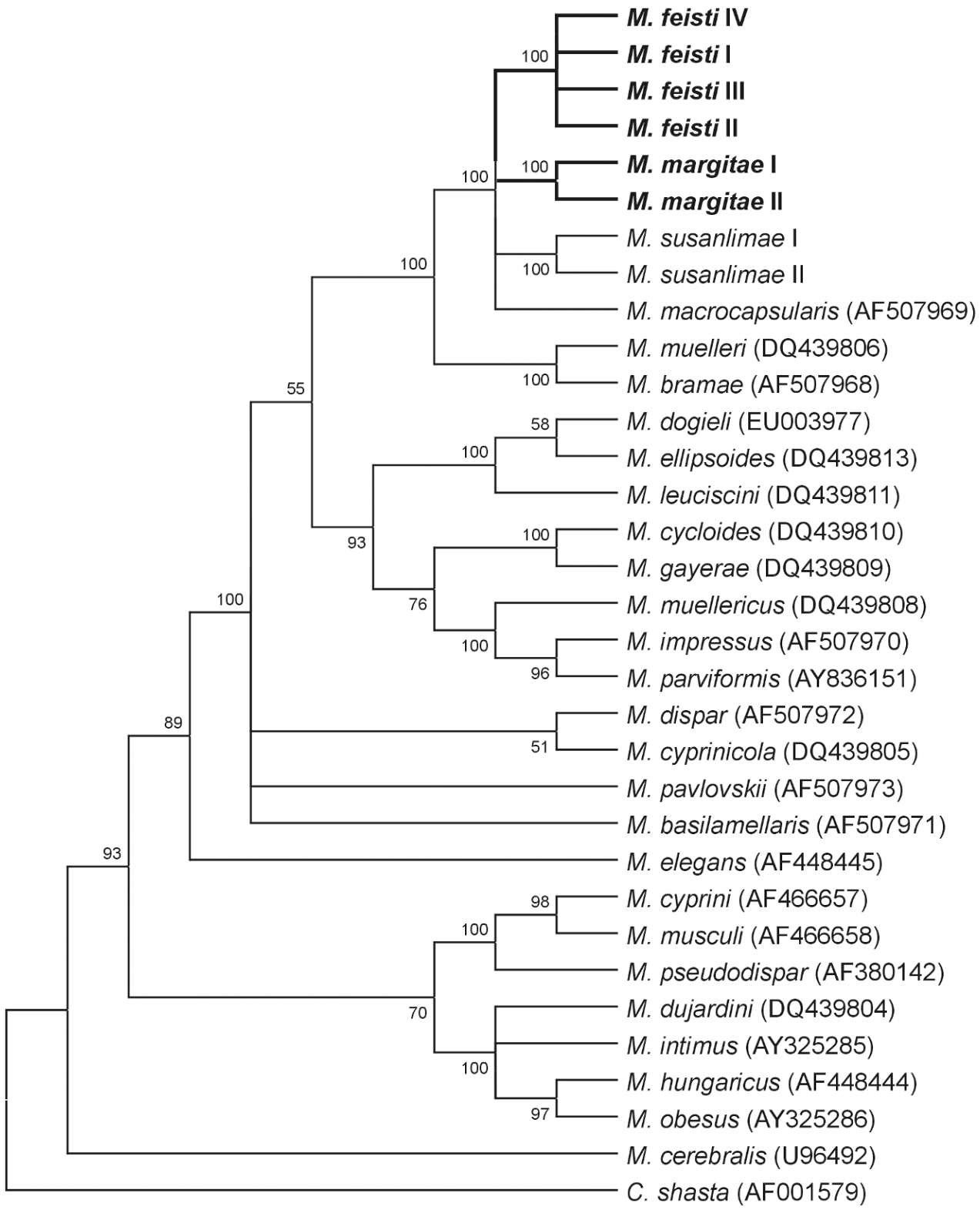

Fig. 11. Phylogenetic tree generated by maximum parsimony of the 18S rDNA sequences of myxosporeans, rooted at *Ceratomyxa shasta*. Numbers at nodes indicate bootstrap confidence values (100 replications). GenBank accession numbers are given in parentheses. Myxosporeans examined in this study are in bold

Type host: Bleak, *Alburnus alburnus* L. (Cyprinidae).

Type locality: River Danube North to Budapest, Hungary (47°39´N, 19°04´E).

Site of tissue development: Cartilaginous rays of the gill filaments.

Type material: Syntype spores in glycerine-jelly were deposited in the parasitological collection of the Zoological Department, Hungarian Natural History Museum, Budapest, Coll. No. HNHM-17831. The 18S rDNA sequence of *M. susanlimae* sp. nov. was deposited in the GenBank under the accession number EU598805.

Prevalence of infection: 22% of the bleak from the Danube.

Etymology: The species is named after Susan Lim Lee Hong, the well known Malaysian fish parasitologist.

Histology: Plasmodia up to 100 µm long and up to 60 µm wide and tightly packed with spores protruded from the 35 to 50 µm wide cartilaginous fin rays in most cases. They had a bright eosinophilic ectoplasm, and at the site where they emerged from the cartilage they were delimited from the basal layers of the gill epithelium by a very thin one-layered connective tissue capsule originating from the perichondrium (Fig. 8). In the infected region the normally straight cartilaginous gill ray became thickened and deformed (Fig. 9).

Molecular data: DNA sequences of two *M. susanlimae* sp. nov. samples (EU598805) from different bleak specimens showed 100% identity based on 1320 aligned base pairs. The species most closely related to *M. susanlimae* sp. nov. was *M. feisti* sp. nov. (Figs 10 and 11) discussed above and reported in this study, showing 97.2% similarity. Another close similarity was found with *M. margitae*, the gill parasite of bleak, which was 97.3% similar to *M. susanlimae* sp. nov.

Remarks: In its size and spore morphology *Myxobolus susanlimae* sp. nov. resembles *M. feisti* sp. nov., but the two species clearly differ in their DNA sequences. *Myxobolus susanlimae* also resembles the specific bleak parasite *M. margitae*, which develops in large plasmodia within the arteries of the gill filaments; however, besides their different histotropism there are clear molecular differences between the two species (EU598803).

Discussion

Most myxosporeans are known to have strict tissue specificity and to select definite sites for their development in the fish body. Some *Myxobolus* species have a specific tropism to cartilaginous tissues. Of these species, Longshaw *et al*. (2003) listed 13 *Myxobolus* spp. (*M. cerebralis*, *M. cartilaginis*, *M. dentium*, *M. divergens*, *M. eucalii*, *M. filamentous*, *M. hoffmani*, *M. hyborhynchi*, *M. indirae*, *M. intrachondrealis*, *M. nuevoleonensis*, *M. petrushewskii* and *M. scleroperca*) from freshwater fishes. Of the above species, only some (e.g. *M. cerebralis*, *M. cartilaginis*, *M. intrachondrealis*) develop among chondrocytes, others (e.g. *M. divergens*, *M. nuevoleonensis*, *M. scleroperca*) prefer cartilaginous-collagenic elements forming bones and fin rays. Both *M. feisti* sp. nov. and *M. susanlimae* sp. nov. belong to the typical chondrophilic species developing among chondrocytes. The cartilaginous gill rays were the only site of development for both species. With their elliptical shape and well-developed triangular appendix, *M. feisti* morphologically resembled *M. susanlimae*; however, besides size differences, there was a difference between the two species also at DNA level, as their 18S rDNA sequences showed only a 97,2% similarity. The both distance algorithm and the maximum parsimony as well as the maximum likelihood (not shown) suggest a clear difference between the two chondrophilic species, supported by high bootstrap levels. The two species seem to be specific to their type hosts. In a similar way, in spore morphology both species resembled *Myxobolus* spp. inhabiting the gill filaments and gill lamellae (*M. muelleri*-type spp. in roach or *M. margitae* in bleak), but they differed from the latter species in their DNA sequences (EU598803). Both species formed nodules and deformities in the cartilaginous gill rays but no severe pathological changes were recorded.

Acknowledgements. The authors thank Ms. Györgyi Ostoros for her help with the histological work and the pencil drawings. The study was rendered possible by the grant of the Hungarian Scientific Research Fund (project no. OTKA K71837).

References

Eszterbauer E. 2004. Genetic relationship among gill-infecting *Myxobolus* species (Myxosporea) of cyprinids: molecular evidence of importance of tissue-specificity. *Diseases of Aquatic Organisms*, 58, 35–40. DOI: 10.3354/dao058035.

Eszterbauer E., Székely Cs. 2004. Molecular phylogeny of the kidney-parasitic *Sphaerospora renicola* from common carp (*Cyprinus carpio*) and *Sphaerospora* sp. from goldfish (*Carassius auratus auratus*). *Acta Veterinaria Hungarica*, 52, 469–478.

Hall T.A. 1999. BioEdit: A user-friendly biological sequence alignment editor and analysis program for Windows 95/98/NT. *Nucleic Acids Symposium Series*, 41, 95–98.

Hillis D.M., Dixon T. 1991. Ribosomal DNA: Molecular evolution and phylogenetic inference. *Quarterly Review of Biology*, 66, 411–453. DOI: 10.1086/417338.

Hoffman G.L., Dunbar C.E., Bradford A. 1962. Whirling disease of trout caused by *Myxosoma cerebralis* in the United States. Specific Scientific Reports. Fish No. 427, 15 pp.

Longshaw M., Frear P., Feist S.W. 2003. *Myxobolus buckei* sp. n. (Myxozoa), a new pathogenic parasite from the spinal column of three cyprinid fishes from the United Kingdom. *Folia Parasitologica*, 50, 251–262.

Molnár K. 1994. Comments on the host, organ and tissue specificity of fish myxosporeans and on the types of their intrapiscine development. *Parasitologica Hungarica*, 27, 5–20.

Molnár K., Eszterbauer E., Székely Cs., Dán Á., Harrach B. 2002. Morphological and molecular biological studies on intramuscular *Myxobolus* spp. of cyprinid fish. *Journal of Fish Diseases*, 25, 643–652. DOI: 10.1046/j.1365-2761.2002.00409.x.

Nowak B., Bruno D., Bryan J. 2001. EAFP. Histopathology Workshops: Notes and Images. Aqua Education; www.aqua.southcom.com.au.

Schäperclaus W. 1931. Die Drehkrankheit in der Forellenzucht und ihre Bekämpfung. *Zeitschrift für Fischerei*, 29, 521–567.

Swofford D.L. 2000. PAUP*. Phylogenetic Analysis Using Parsimony (*and Other Methods). Version 4. Sinauer Associates, Sunderland, Massachusetts.

Tamura K., Dudley J., Nei M., Kumar S. 2007. MEGA4: Molecular Evolutionary Genetics Analysis (MEGA) software version 4.0. *Molecular Biology and Evolution*, 24, 1596–1599. DOI: 10.1093/molbev/msm092.

Thompson J.D., Higgins D.G., Gibson T.J. 1994. CLUSTAL W: improving the sensitivity of progressive multiple sequence alignment through sequence weighting, position-specific gap penalties and weight matrix choice. *Nucleic Acids Research*, 22, 4673–4680. DOI: 10.1093/nar/22.22.4673.

(Accepted September 5, 2008)